X Encontro Brasileiro sobre Adsorção
27 a 30 de Abril de 2014
Guarujá - SP

MASS TRANSFER MODELS FOR THE ADSORPTION OF ACID RED 357 AND ACID BLACK 210 BY TANNERY SOLID WASTES.

J. S. Piccin[1]; M. Gutterres[2]; M. Schwaab[3]; G. L. Dotto[3]

1- Food Engineering – Passo Fundo University
Br. 285, Km 171 – CEP: 99052-900 – Passo Fundo- RS – Brazil
Email: jefersonpiccin@gmail.com
2- Chemical Engineering Department – Federal University of Rio Grande do Sul
Luiz Englert Street, s/n° – CEP: 90040-040 – Porto Alegre- RS – Brazil
Email: mariliz@enq.ufrgs.br
3- Chemical Engineering Department – Federal University of Santa Maria
Roraima Avenue, 1000 – CEP: 97105-900 – Santa Maria- RS – Brazil
Email: guilherme_dotto@yahoo.com.br

ABSTRACT: In this work, diffusional mass transfer models with and without external resistance were applied to represent the adsorption of Acid Red 357 (AR357) and Acid Black 210 (AB210) by tannery solid wastes. Adsorption kinetic curves were obtained at different temperatures (288, 298 and 308 K) and represented according to the models. The mass transfer parameters, such as, external mass transfer coefficient (k_f) and surface diffusion coefficient (D_s) were evaluated. The two models agreed with the experimental data, but, very higher values of k_f were obtained using the model with external resistance. This indicated that the external mass transfer mechanism can be neglected. Then the model without external resistance, which is simpler, can be used.

KEYWORDS: Adsorption; parameter estimation; external mass transfer; surface diffusion.

1. INTRODUCTION

Colored effluents are a direct result of the dyes production, and also, consequence of its use in the textile and related industries (Noroozi and Sorial, 2013). It is estimated that about 40-65 L of textile effluent are generated per kg of cloth produced (Mezohegyi *et al.*, 2012). The inadequate release of these colored effluents in aqueous ecosystems is esthetically unpleasant and leads to a reduction in sunlight penetration, which in turn decreases photosynthetic activity, dissolved oxygen concentration, and water quality. Furthermore, had acute toxic effects on aquatic flora and fauna, causing severe environmental problems worldwide (Saratale *et al.*, 2011). This scenario shows the importance of the treatment of dye containing effluents, prior to their final discharge into the environment.

Several technologies for dyes removal from effluents are presented in the literature (Gupta and Suhas, 2009; Srinivasan and Viraraghavan, 2010; Saratale *et al.*, 2011; Mezohegyi *et al.*, 2012). Among all of these, adsorption has been preferred due to its cheapness and high-quality of the treated effluents, especially for well-designed processes (Salleh *et al.*, 2011). The main used adsorbent in dye removal is activated carbon, but, the use of cheap and eco-friendly materials have been studied as alternatives (Demirbas, 2009). Recently, tannery solid wastes were successfully employed for dyes adsorption, proving some advantages, for example, the reuse of the treated water in leather industry (Piccin *et al.*, 2012, 2013). However, more detailed studies about the mass transfer mechanism in the dyes adsorption onto tannery solid wastes are still necessary.

In solid-liquid adsorption systems, the mass transfer mechanism occurs by external mass transfer, intraparticle diffusion (pore volume diffusion, surface diffusion, or a combination of both mechanisms) and adsorption on the active sites (Ruthven, 1984; Suzuki, 1990). The diffusional mass transfer models are constructed on the basis in the above mentioned steps (Ocampo-

Pérez *et al.*, 2010, 2011, 2012). In this way, these models can be used as realistic Physico-mathematical tolls to elucidate the dyes adsorption onto tannery solid wastes.

This work aimed to develop diffusional mass transfer models with and without external resistance to represent the adsorption of AR357 and AB210 by tannery solid wastes. The models were based on the mass transfer principles and used to represent the adsorption kinetic curves under different temperatures (288, 298 and 308 K). The values of k_f and D_s were estimated and its dependence with the temperature was studied. The rate limiting step of the adsorption process was also elucidated.

2. EXPERIMENTAL SECTION

2.1. Obtainment of the Tannery Solid Wastes

Tannery solid wastes (TSW) were obtained from chromium-tanned leather shaving operation in a o-RS, Brazil). These residues were dried under vacuum conditions (-500 mmHg) at 60 ◦C for 48 h (Piccin *et al.*, 2012). TSW were cut in rectangular shape (3.31 x 3.31 mm) with thickness of 0.50 mm.

2.2. Characterization Techniques

TSW were characterized according to the moisture content (ASTM D3790-79) solid density (ρ_s) (picnometry), void fraction (ε_p) and surface area (S) (BET method) (Quantachrome Instruments, New Win 2, USA) (Dotto and Pinto, 2012). Scanning electron microscopy (SEM) (Jeol, JSM-6060, Japan) was used to observe the TSW surface. The main elements on the TSW surface were identified by energy dispersive X-ray spectroscopy (Jeol, JSM 5800, Japan).

2.3. Dyes

Acid Red 357 (AR357) (azo-dissulphonated Cr organic-complex dye, molecular weight 956.7 g mol^{-1}, CAS 57674-14-3, λ_{max} = 494 nm) and Acid Black 210 (AB210) (amine dissulfonated triazo organic dye, molecular weight 965.9 g mol^{-1}, CAS 99576-15-5, λ_{max} = 459 nm) were supplied by the Business Leather Unit of Lanxess Company. The chemical structures of the dyes are shown in Figure 1. Distilled water was used to prepare all solutions. All reagents were of analytical-grade.

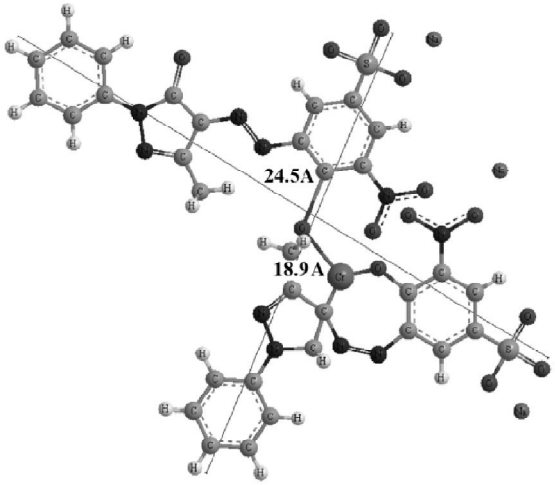

(a)

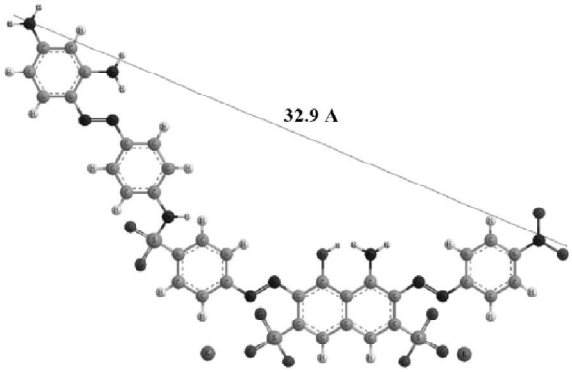

(b)

Figure 1. Optimized three-dimensional chemical structures of (a) AR357 and (b) AB210.

2.4. Adsorption Assays

The adsorption kinetic assays were carried out in batch conditions at different temperatures (288, 298 and 308 K) using a thermostated shaker (Nova etica, 218 MBD, Brazil). 0.25 g of TSW (dry basis) was added to 10 mL of citric acid/sodium diphosphate buffer (0.1 mol L^{-1}) at pH 2.5. After 10 min, 50 mL of dye aqueous solution (with desired concentrations) was added and the system was stirred at 150 rpm and at a controlled temperature. Aliquots were withdrawn in preset time intervals and the dye remaining concentration was determined by spectrophotometry (Varian, Cary 100, USA). All adsorption experiments were performed in duplicate (n=2).

3. MODEL DEVELOPMENT

The mathematical model was developed according to the mass balances in the liquid phase, describing the variation of dye concentration along the time (Equation 1), and in the solid phase, describing the variation of dye concentration along the time and in the solid position (Equation 2) (Ruthven, 1984; Suzuki, 1990). Low values of void fraction (ε_p) were observed for the adsorbent, so, it can be assumed that the surface diffusion is the predominant intraparticle mass transfer mechanism. The initial and boundary conditions are presented in the Equations 3, 4 and 5:

$$\frac{dC_B}{dt} = -\frac{1}{L}\frac{V_S}{V_L} k_f \left(C_B - C_S\right) \quad (1)$$

$$\frac{\partial q}{\partial t} = D_S \frac{\partial^2 q}{\partial z^2} \quad (2)$$

$$t = 0\,,\ 0 \le z \le L \Rightarrow q = 0 \quad (3)$$

$$\left.\frac{\partial q}{\partial z}\right|_{z=0} = 0 \quad (4)$$

$$\rho_S D_S \left.\frac{\partial q}{\partial z}\right|_{z=L} = k_f \left(C_B - C_S\right) \quad (5)$$

In Equations 1 to 5, C_B is the liquid bulk concentration (mg L^{-1}), C_S is the liquid phase concentration at solid-liquid interface (mg L^{-1}), q is the concentration in the solid phase (mg g^{-1}), L is the half of the adsorbent thickness (m), V_S and V_L are solid and liquid volumes (m^3), k_f is the external mass transfer coefficient (m s^{-1}), D_S is the surface diffusion coefficient (m^2 s^{-1}), ρ_S is the solid density (g m^{-3}), t is time (s) and z corresponds to the solid position (m).

The equations are connected through the external mass transfer from the bulk liquid phase to the solid surface. The liquid concentration at surface C_S was considered to be in equilibrium with the adsorbed phase concentration at solid surface. The equilibrium relations are defined according to the Langmuir isotherm (Equation 6) for Acid Red 357 and BET model (Equation 7) for Acid Black 210. The values of q_m, k_L, q_{BET}, k_1 and k_2 for different temperatures can be found in Piccin *et al.* (2013).

$$q(t,L) = \frac{q_m k_L C_S}{1 + k_L C_S} \quad (6)$$

$$q(t,L) = \frac{q_{BET} k_1 C_S}{\left(1 - k_2 C_S\right)\left(1 - k_2 C_S + k_1 C_S\right)} \quad (7)$$

The model presented in Equations 1 to 5 can be simplified when the external mass transfer is very fast. In this case, the value of the external mass transfer coefficient k_f reach very high values and C_S is equal C_B. Then, the Equation 5 is reduced to Equation 12. By the other side, the external mass transfer term in Equation 1 is changed by the diffusive mass transfer term, as presented in Equation 8. Equations 2, 3 and 4 that describe the solid volume are not changed and are rewritten in Equations 9, 10 and 11:

$$\frac{dC_B}{dt} = -\frac{1}{L}\frac{V_S}{V_L} \rho_S D_S \left.\frac{\partial q}{\partial z}\right|_{z=L} \quad (8)$$

$$\frac{\partial q}{\partial t} = D_S \frac{\partial^2 q}{\partial z^2} \quad (9)$$

$$t = 0\,,\ 0 \le z \le L \Rightarrow q = 0 \quad (10)$$

$$\left.\frac{\partial q}{\partial z}\right|_{z=0} = 0 \quad (11)$$

$$C_S = C_B \quad (12)$$

The partial differential equations were discretized with respect to z coordinate through orthogonal collocation method (Villadsen and Michelsen, 1978; Pinto and Lage, 2001). The resulting system of ordinary differential equations was solved with the help of DASSL code (Petzold *et al.*, 1989).

In order to allow the models evaluation at different temperatures simultaneously, D_S was considered a function of the temperature, according to the Equation 13 (Schwaab and Pinto, 2007):

$$D_S = D_{S,Tref} \exp\left[B\left(\frac{T - T_{ref}}{T}\right)\right] \quad (13)$$

In Equation 13, $D_{S,Tref}$ (m^2 s^{-1}) is the surface diffusional coefficient at reference temperature T_{ref} (in this work, T_{ref} value was equal to 298 K), B is a parameter that describes how surface diffusional coefficient varies with temperature T. The

dependence of k_f with T was found to be negligible and a constant value for all temperature was estimated.

The parameters $D_{S,ref}$, B and k_f were simultaneously estimated through minimization of the least squares function presented in Equation 14:

$$S = \sum_{i=1}^{N} \left(C_B^{\exp} - C_B^{\mathrm{mod}} \right)^2 \qquad (14)$$

The minimization of Equation 14 was performed by a hybrid optimization algorithm, composed by Particle Swarm Optimization and a Newton-like optimization method (Schwaab *et al.*, 2008).

4. RESULTS AND DISCUSSION

4.1. Adsorbent Characteristics

The moisture content of TSW was 7.8±0.8% (wet basis). The solid density, void fraction and surface area were, respectively, 1450±37 kg m^{-3}, 15±2% and 3.23±0.63 m^2 g^{-1}. The main elements on the TSW surface were C, N, O and Cr. The SEM image of the adsorbent is shown in Figure 2.

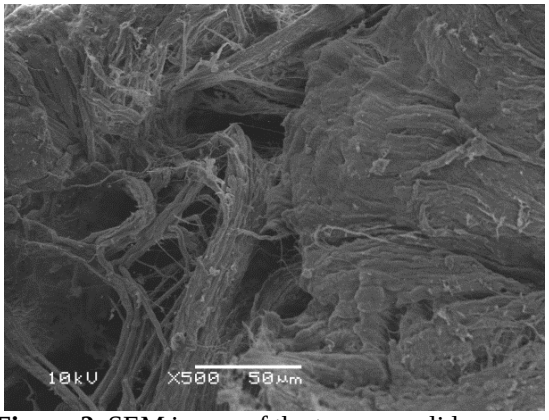

Figure 2. SEM image of the tannery solid wastes.

Figure 2 reveals a complex, non porous and heterogeneous surface of TSW. Some interlaced fibers can be observed. This interlacement suggests a lower void fraction and surface area, as demonstrated by BET analysis. Furthermore, on the basis in these structural characteristics, it can be inferred that the large dye molecules are transferred mainly by surface diffusion in the solid phase.

4.2. Model Parameters

The experimental data of batch adsorption of Acid Red 357 and Acid Black 210 on tannery solid wastes at three different temperatures were used for the estimation of the mass transport parameters. During the parameters estimation of Acid Black 210, it was observed that the experimental data at 288 K present a strange behavior, since adsorption rate is higher than the values observed at 298 K. For this reason, adsorption data of Acid Black 210 at 288 K were not considered. In Figures 3 and 4, are presented the model adjustment to the experimental data of Acid Red 357 and Acid Black 210, respectively.

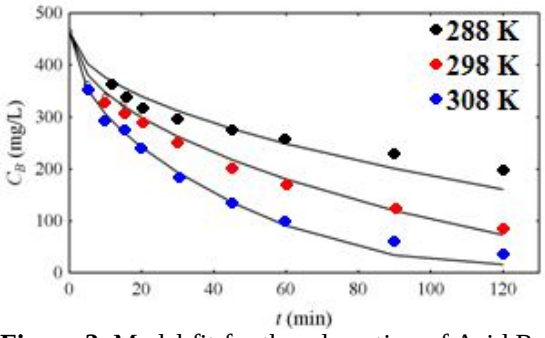

Figure 3. Model fit for the adsorption of Acid Red 357 at different temperatures.

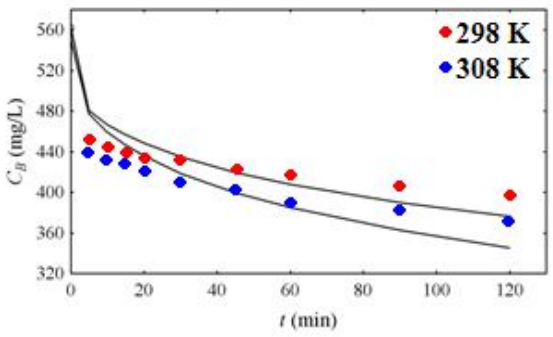

Figure 4. Model fit for the adsorption of Acid Black 210 at different temperatures.

.

In Figure 3, it can be seen that model quality is relatively good, but, the model adjustment to the experimental data in Figure 4 is not quite satisfactory. In this case, a very high adsorption rate is observed at five initial minutes. After this initial period, adsorption rate is very low and very similar at two different temperatures, since the slopes of experimental data are identical.

The estimated parameters are presented in Table 1. It can be clearly observed in Table 1 that

the external mass transfer coefficients k_f are very high, since the usual values ranging from 10^{-6} to 10^{-3} m s^{-1} (Suzuki, 1990). This indicates that the external mass transfer resistance can be readily neglected. This fact justifies the use of the simplified model presented in Equations 8-12.

Table 1. Estimated parameters for batch adsorption of both dyes.

Parameter	Acid Red 357	Acid Black 210
k_f (m s^{-1})	1.00	1.00
$D_{S,Tref}$ (m^2 h^{-1})	4.49×10^{-9}	0.384×10^{-9}
B	13.6	11.5

Since that the model without external resistance was physically adequate, the two parameters that describe how the surface diffusion coefficient varies as a function of temperature (Equation 13) were estimated and nonlinear confidence regions were constructed (Schwaab *et al.*, 2008). The confidence region of the parameters is shown in Figures 5 and 6.

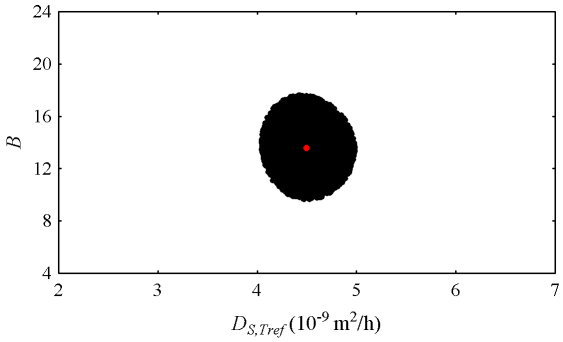

Figure 5. Confidence region of the estimated parameters with the simplified model for Acid Red 357.

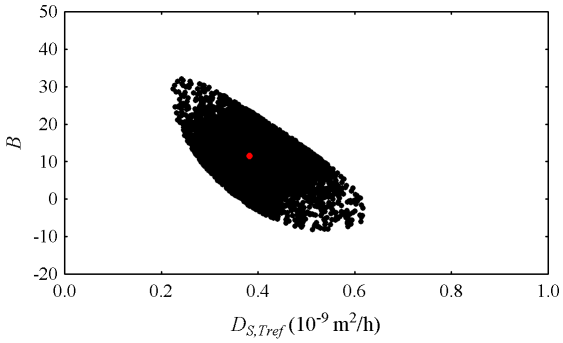

Figure 6. Confidence region of the estimated parameters with the simplified model for Acid Black 210.

In fact, the estimated parameters (indicated as red points in Figures 5 and 6) are equal to the ones presented in Table 1, as it could be expected. Figure 5 shows that both parameters are very well identified, with low parameter uncertainties. Besides, Figure 5 shows that parameter B presents a high level of uncertainty. Also, confidence interval includes positive and negative values. It is important to recall that parameter B defines how surface diffusion coefficient varies with temperature. This result indicates that an increase in the temperature causes a small increase in the surface diffusion coefficient, which is not significant when compared to the experimental uncertainty.

Besides, Figure 5 shows that parameter B presents a high level of uncertainty. Also, confidence interval includes positive and negative values. It is important to recall that parameter B defines how surface diffusion coefficient varies with temperature. This result indicates that an increase in the temperature causes a small increase in the surface diffusion coefficient, which is not significant when compared to the experimental uncertainty.

The D_s values ranged from 0.79×10^{-12} to 1.94×10^{-12} m^2 s^{-1} for Acid Red 357 and from 0.11×10^{-12} to 0.16×10^{-12} m^2 s^{-1} for Acid Black 210. These values are in accordance with the values reported in the literature for surface diffusion coefficient (Ruthven, 1984; Ocampo-Pérez *et al.*, 2010, 2011, 2012). It can be noted that the D_s values for Acid Red 357 were higher than the D_s values for Acid Black 210. This probably occurred because the dye dimensions (see Figure 1). Acid Black 210 molecular size is higher than Acid Red 357 molecular size, hindering its transference within the adsorbent and leading to lower values of D_s.

5. CONCLUSION

Mass transfer mathematical models were used to represent the adsorption data of Acid Red 357 and Acid Black 210 dyes onto tannery solid wastes. Experiments were performed at three different temperatures. Initially, the use of a model with external and internal mass transfer resistances were employed to fit the experimental data and the results showed that external mass transfer resistance is negligible. In this way, the model without external resistance, which is simpler, can

be used. The estimated values for surface diffusion coefficient ranged from 0.79×10^{-12} to 1.94×10^{-12} m^2 s^{-1} for Acid Red 357 and from 0.11×10^{-12} to 0.16×10^{-12} m^2 s^{-1} for Acid Black 210 and are in accordance with literature. This indicates that the internal mass transfer is the rate limiting step in the adsorption of dyes onto tannery solid wastes.

6. REFERENCES

DEMIRBAS, A. Agricultural based activated carbons for the removal of dyes from aqueous solutions: A review. *J. Hazard. Mater.*, v. 167, p. 1-9, 2009.

DOTTO, G. L.; PINTO, L. A. A. Analysis of mass transfer kinetics in the biosorption of synthetic dyes onto *Spirulina platensis* nanoparticles. *Biochem. Eng. J.*, v. 68, p. 85-90, 2012.

GUPTA, V. K.; SUHAS. Application of low-cost adsorbents for dye removal: A review. *J. Environ. Manage.*, v. 90, p. 2313-2342, 2009.

MEZOHEGYI, G.; VAN DER ZEE, F. P.; FONT, J.; FORTUNY, A.; FABREGAT, A. Towards advanced aqueous dye removal processes: A short review on the versatile role of activated carbon. *J. Environ. Manage.*, v. 102, p. 148-164, 2012.

NOROOZI, B.; SORIAL, G. A. Applicable models for multi component adsorption of dyes: A review. *J. Environ. Sci.*, v. 25, p. 419-429, 2013.

OCAMPO-PEREZ, R.; LEYVA-RAMOS, R.; ALONSO-DAVILA, P.; RIVERA-UTRILLA, J.; SÁNCHEZ-POLO, M. Modeling adsorption rate of pyridine onto granular activated carbon. *Chem. Eng. J.*, v. 165, p. 133-141, 2010.

OCAMPO-PEREZ, R.; LEYVA-RAMOS, R.; MENDOZA-BARRON, J.; GUERRERO-CORONADO, R. M. Adsorption rate of phenol from aqueous solution onto organobentonite: Surface diffusion and kinetic models. *J. Colloid Interface Sci.*, v. 364, p. 195-204, 2011.

OCAMPO-PÉREZ, R.; RIVERA-UTRILLA, J.; GÓMEZ-PACHECO, C.; SÁNCHEZ-POLO, M.; LÓPEZ-PEÑALVER, J. J. Kinetic study of tetracycline adsorption on sludge-derived adsorbents in aqueous phase. *Chem. Eng. J.*, v. 213, p. 88-96, 2012.

PETZOLD, L. R. *DASSL Code (Differential Algebraic System Solver)*, Computing and Mathematics Research Division, Lawrence Livermore National Laboratory, Livermore, CA, USA, 1989.

PICCIN, J. S.; FERIS, L. A.; COOPER, M.; GUTTERRES, M. Dye Adsorption by Leather Waste: Mechanism Diffusion, Nature Studies, and Thermodynamic Data. *J. Chem. Eng. Data*, v. 58, p. 873-882, 2013.

PICCIN, J. S.; GOMES, C. S.; FERIS, L. A.; GUTTERRES, M. Kinetics and isotherms of leather dye adsorption by tannery solid waste. *Chem. Eng. J.*, v. 183, p. 30-38, 2012.

PINTO, J. C.; LAGE, P. L. *Métodos numéricos em problemas de engenharia química*. Rio de Janeiro: Editora e-Papers, 2001.

RUTHVEN, D. M. *Principles of Adsorption and Adsorption Processes*. New York: John Wiley & Sons, 1984.

SALLEH, M. A. M.; MAHMOUD, D. K.; ABDUL KARIM, W. A. W.; IDRIS, A. Cationic and anionic dye adsorption by agricultural solid wastes: A comprehensive review. *Desalination*, v. 280, p. 1-13, 2011.

SARATALE, R. G.; SARATALE, G. D.; CHANG, J. S.; GOVINDWAR, S. P. Bacterial decolorization and degradation of azo dyes: A review. *J. Taiwan Inst. Chem. Eng.*, v. 42, p. 138-157, 2011.

SCHWAAB, M.; BISCAIA JR., E. C.; MONTEIRO, J. L.; Pinto, J. C. Nonlinear parameter estimation through particle swarm optimization. *Chem. Eng. Sci.*, v. 63, p. 1542-1552, 2008.

SCHWAAB, M.; PINTO, J. C. Optimum reference temperature for reparameterization of the Arrhenius equation. Part 1: problems involving one kinetic constant. *Chem. Eng. Sci.*, v. 62, p. 2750-2764, 2007.

SRINIVASAN, A.; VIRARAGHAVAN, T. Decolorization of dye wastewaters by biosorbents:

A review. *J. Environ. Manage.*, v. 91, p. 1915-1929, 2010.
SUZUKI, M. *Adsorption Engineering*. Tokyo: Kodansha, 1990.

VILLADSEN, J.; MICHELSEN, M. L. *Solution of Differential Equation Models by Polynomial Approximation.* New Jersey: Pretence-Hall Inc., 1978.